

Corrosion model for Zircaloy-4 cladding in PWR

Byung-Ho LEE, Yeon-Jong YOO, Yang-Hyun KOO and Dong-Seong SOHN
Korea Atomic Energy Research Institute
150 Duckjin-dong Yusong-gu Taejeon, Korea 305-353
Email : bhlee2@kaeri.re.kr

ABSTRACT

To improve the corrosion model of the fuel performance analysis code COSMOS, a model was developed considering thermohydraulic phenomena and the effect of water chemistry and low Sn in the alloy composition on the corrosion behavior. It is assumed that the lithium enhancement factor influences the corrosion behavior only if the subcooled void is present in the coolant.

The developed model was verified with the database obtained from Grohnde and Ringhals 3 reactors. Comparison of predicted oxide thickness with measured data showed the applicability of COSMOS code to analyze the cladding oxidation.

In the future, the effect of the hydride in the cladding and the precipitate changes due to irradiation should be included.

1. INTRODUCTION

Corrosion of Zircaloy cladding in PWR has become more important because of (1) higher fuel discharge burnup to reduce fuel cycle costs, (2) higher coolant inlet temperature to increase plant thermal efficiency, and (3) increase of coolant pH and lithium concentration to reduce plant radiation levels.

Even though the corrosion mechanism of Zircaloy is still not well understood, the main factors determining the corrosion rate are fast neutron flux, thermal conductivity of zirconia, alloy composition, water chemistry, and thermohydraulic condition.

High neutron flux affects the structure of the oxide films on Zircaloy cladding and the chemistry within pores in the oxide so the change of oxide is expected to accelerate the Zircaloy corrosion depending on the intensity of neutron flux.

Concerning on water chemistry, Shann [1] and Billot [2] have observed an increase corrosion rate of approximately 10 to 30 % when the maximum coolant lithium contents from 2.2 to 3.5 ppm. On the contrary, results from HALDEN [3,4] and Ringhals 3 [5] showed the presence of lithium had produced no enhancement in oxidation. On the contrary, it has been reported that the presence of boric acid slows down the corrosion behavior.

Phenomenological corrosion model for Zircaloy-4 cladding was developed to account for the irradiation effect, the tin contents in the cladding alloy, and

lithium and boron effect coupled with void fraction in the coolant.

Model verification was carried by some measured cladding oxide layer thickness data obtained from PWRs.

2. DESCRIPTION OF CORROSION MODEL

The oxidation process of Zircaloy cladding can generally be estimated using semi-empirical correlations divided by pre-transition and post-transition kinetics.

The Zircaloy corrosion process being essentially a diffusion-controlled reaction for all the semi-empirical models, Zircaloy oxidation kinetics are presented by Arrhenius equation as a function of temperature, activation energy and additional acceleration effects.

In the oxide layer thickness range up to around 2.1 μm (pre-transition range), oxide layer formation has a cubic characteristic. At a layer thickness above 2.1 μm there is a change to the linear corrosion kinetics. Oxide layer formation during the pre-transition is very compact and protective tetragonal structure, and has black and lustrous color, whereas the oxide after pre-transition becomes friable and gray monoclinic structure.

The corrosion rate equation in the pre-transition regime is given by

$$\frac{ds^3}{dt} = K_{pre} \cdot \exp\left(-\frac{Q_{pre}}{R \cdot T_i}\right) \quad (\text{mm}^3/\text{day})$$

$$K_{pre} = F_{Sn} \cdot F_{Li,pre} \cdot F_B \cdot F_{pre}$$

while the oxidation rate in the post-transition regime is given by

$$\frac{ds}{dt} = K_{post} \cdot \exp\left(-\frac{Q_{post}}{R \cdot T_i}\right) \quad (\text{mm}/\text{day})$$

$$K_{post} = (K_1 + K_2 \cdot (K_3 \cdot \mathbf{f})^{K_4}) \cdot F_{Sn} \cdot F_{Li,post} \cdot F_B \cdot F_{post}$$

where

s = oxidation thickness [mm]

t = time [day]

R = gas constant [cal/mol-K]

T_i = metal/oxide interface temperature [K]

K_{pre} = frequency factor for pre-transition regime [mm³/day]

K_{post} = frequency factor for post-transition regime [mm/day]

Q_{pre} = activation energy for pre transition = 32,289 [cal/mol-K]

Q_{post} = activation energy for pre transition = 27,354 [cal/mol-K]

- $F_{Li,pre}$ = enhancement factor due to lithium in the pre-transition regime
 $F_{Li,post}$ = enhancement factor due to lithium in the post-transition regime
 F_B = boron effect factor
 F_{Sn} = tin content enhancement factor
 ϕ = fast neutron flux (> 0.821 MeV) [n/cm²-s]
 K_1, K_2, K_3, K_4 = constants to determine the irradiation enhancement factor

2.1 Tin effect

Improved low-tin cladding of which tin content ranges from 1.2 to 1.4 wt% shows the reduction of the oxide thickness at high burnups by about 20 to 40% even though the role of tin in the oxide growth mechanism is not clear.

The high burnup oxide measurements studied in this model included for cladding with low tin content and standard tin content. By using corrosion data from GROHNDE and GOESGEN reactors, these phenomena can be expressed by a multiplicative coefficient included in the frequency factor.

$$F_{Sn} = 0.7 \quad \text{for low tin cladding}$$

$$F_{Sn} = 1.0 \quad \text{otherwise}$$

2.2 Lithium Hydroxide Exposure

LiOH at a lithium concentration of less than ~2.5 ppm has been generally used in PWRs at startup to maintain the coolant pH within 6.9 to 7.4 in order to control the corrosion of primary system materials and minimize corrosion product transport within the primary system. The lithium concentration normally decreases in coordination with decreasing boric acid concentration as time progresses and is normally reduced to ~0.6 ppm at the end of a fuel cycle when the boron concentration depleted. For longer fuel cycle operations with higher startup lithium concentration has been of interest to fuel users. Corrosion models by Sabol and Billot have attributed a significant portion of in reactor Zircaloy cladding corrosion to an enhancement effect of lithium. However, recent assessment of corrosion data taken from several plants operated with various startup concentration of lithium, ranging from 2.2 to 3.5ppm, have indicated no easily discernible effect of lithium on Zircaloy cladding corrosion when operated to an oxide thickness of less than 70 μ m in PWRs.

Laboratory and ex-reactor heat transfer loop studies of the effects of lithium hydroxide/boric acid additions on Zircaloy-4 corrosion have been reported. Evidence from these studies for a lithium-related acceleration under PWR water chemistry is somewhat conflicting. In loop tests in the core of the Halden test reactor (4.0 to 45 ppm lithium, 700 to 1000 ppm B, and 1.0% voids), no remarkable effect of lithium on Zircaloy cladding corrosion was observed. On the contrary, Billot [2] and Cheng [6] reported the lithium enhanced corrosion rate.

Even though it needs more discussion on the effect of Lithium on corrosion rate, the KAERI's corrosion model postulates(?) the lithium enhanced corrosion rate if the void fraction in the coolant is formed enough to concentrate the lithium in the cladding surface.

Then the formulation of a lithium history-dependent enhancement factor is given by

$$F_{Li} = (1 + \mathbf{a}) \cdot f([Li], T, f)$$

$$F_{Li} = \begin{cases} 1.0 & \text{if } \mathbf{a} \leq 0.0\% \\ F_{Li} & \text{if } \mathbf{a} > 0.0\% \end{cases}$$

where

f = fitting constant

α = void fraction

$[Li]$ = Lithium concentration [ppm]

2.3 Estimation of void fraction, \mathbf{a}

Void fraction can be specified by homogeneous model such as

$$\mathbf{a} = 0 \quad X_t \leq 0$$

$$\mathbf{a} = \frac{X_t v_g}{(1 - X_t) v_f + X_t v_g} \quad X_t > 0$$

where

X_t = true quality

n_f = specific volume of saturated liquid [J/kg-K]

n_g = specific volume of saturated vapor [J/kg-K]

Subcooled formation can be estimated by using Levy's subcooled void model [7,8]. Levy's model calculates the true quality in terms of the equilibrium quality and the quality at which bubble departure starts. It is given by:

$$X_t = 0 \quad X_e < X_d$$

$$X_t = X_e - X_d \exp\left(\frac{X_e}{X_d} - 1\right) \quad X_e \geq X_d$$

where

X_e = equilibrium quality

X_d = quality at the point of bubble departure

2.4 Boron effect

It has been observed experimentally that the presence of boric acid in the coolant slows down Zircaloy corrosion kinetics. Cox et al. [9] proposed that H_3BO_3 in combination with LiOH might form a complex salt of $Li_xZr_yB_zO_n$ which appears to plug pores in the oxide and thereby effectively prevent the development of deep pores. The boron effect on corrosion behavior is expressed by [10]

$$F_B = 0.64 \quad \text{if } \alpha \geq 0.0\% \text{ in the presence of Boron}$$

$$F_B = 1.0 \quad \text{otherwise}$$

3. RESULTS AND DISCUSSION

The corrosion model is implemented in the fuel performance code, COSMOS [11] for evaluation of cladding corrosion behavior in PWRs.

The developed corrosion model is verified by experimentally measured database from the 2 case fuel rods irradiated in GROHNDE and RINGHALS-3 PWRs.

3.1 CASE 1 (GROHNDE)

The cladding materials were standard and low tin Zircaloy-4 with average tin contents of 1.5 and 1.3 wt%, respectively. The nominal thermal hydraulic parameters of GROHNDE PWR are listed in Table 1 [12]. The plant was operated for all four cycles with a nominal pH of 7.3. The maximum lithium hydroxide concentration at beginning-of-cycle was 2.0 ppm Li.

Typical oxide thickness layers for standard and low Sn cladding as a function of axial rod position at a given end of operation cycle are compared with the measured data in Fig. 1 and 2, respectively. The oxide layer thickness measurements were carried out by the edge current probe technique. In these calculations the fuel rod has been divided into 20 axial segments. It is noted that low Sn Zircaloy is appreciably more corrosion resistant than high Sn Zircaloy, i.e. the peak oxide layer thicknesses of standard and low-Sn cladding were 80 and 40 μm , respectively. Given the complexity of the condition, the agreement between the measurements and calculation is satisfactory.

In addition, it is noteworthy that some fuel rods are irradiated at very high linear heat generation rate in the beginning-of-cycle. Therefore, the lithium concentration has influence on the corrosion kinetics based on the assumption that the lithium combined with the effect of void in the coolant enhances the corrosion rate as shown in Fig. 3.

Table 1. Design thermal hydraulic parameters of GROHNDE

	Original power	Uprated power*
Nominal thermal power	3765 MW	3850 MW
Number of coolant pumps	4	4
Coolant flow rate (including bypass)	27.17 m ³ /s	27.12 m ³ /s
Core bypass percentage	6 %	6 %
Fraction of heat produced in fuel pin	98 %	98 %
Average linear heat generation rate	207.0 W/cm	212.0 W/cm
Primary coolant pressure	158 bar	158 bar
Average coolant temperature	308.7 °C	309.6 °C
Coolant inlet temperature	291.5 °C	292.1 °C
Coolant outlet temperature	325.9 °C	327.2 °C

* The nominal power was updated in January 1990

3.2 CASE 2 (RINGHALS)

The corrosion model predictions have been compared against many oxide thickness data point for Zircaloy-4 cladding irradiated in RINGHALS-3. The RINGHALS-3 reactor is a 3-loop plant operating with 17×17 fuel assemblies at high LiOH concentrations (maximum 3.5 ppm). Nominal fuel rod and reactor data are listed in Table 2 and 3 [13]. Test rods reached an assembly average burnup of around 40 MWd/kgU.

Table 2. Fuel rod data of RINGHALS 3 cladding

Assembly Type	17×17
Pellet outside diameter	8.19 mm
Cladding outer diameter	9.50 mm
Cladding inner diameter	8.36 mm
Active fuel length	3.6576 m
Rod pitch	12.6 mm

Table 3. Main Core Data of RINGHALS 3 reactor

Average power density	178.0 W/cm
System pressure	15.51 MPa
Coolant flow rate	3510 kg/m ² -s
Coolant inlet temperature	285 °C
Coolant outlet temperature	322 °C

For the considered rods, typical predicted versus measured data for the end-cycle peak oxide layer thickness shows the good agreement as shown in Fig. 4.

3.3 Summary of corrosion model verification

Fig. 5 shows the summary of predicted versus measured data from GROHNDE and RINGHALS-3 experiments. It is well known that a large scattering in the Zircaloy oxide layer thickness is obtained not only from one reactor to another but also within the same reactor with rods manufactured by the same process

and experiencing similar irradiation histories. However, the developed corrosion model implemented in COSMOS code well predicts the various corrosion behaviors.

4. CONCLUSION

Phenomenological corrosion model for Zircaloy-4 cladding was developed to account for the irradiation effect, the tin contents in the cladding alloy, and lithium and boron effect coupled with void fraction in the coolant. The Sn effect is considered by analyzing the measured corrosion data from GROHNDE and GOESGEN reactors. It is assumed that water chemistry condition such as boron and lithium contents can have influence on the corrosion behavior under the condition of the subcooled void formation in the coolant.

The corrosion model implemented in the fuel performance code COSMOS was verified with cladding corrosion data from GROHNDE and RINGHALS-3 plants.

Comparison of predicted oxide thickness with measured data showed the good agreement and the ability of COSMOS code to analyze the cladding oxidation.

Acknowledgements

The authors would like to express their appreciation to the Ministry of Science and Technology (MOST) of the Republic of Korea for the support of this work through the mid- and long-term nuclear R&D Project.

Reference

1. S.H. Shann, L.F. van Swarn and L.A. Martin, "Effects of Coolant Li Concentration on PWR Cladding Waterside Corrosion", Proceedings of the International Topical Meeting on LWR Fuel Performance, Avignon, France, April 21-24, 1991, pp. 742-748.
2. P. Billot, J. Robin, A. Giordano, J. Peybernes, J. Thomazet and H. Amaulrich, "Experimental and Theoretical Studies of Parameters that Influence Corrosion of Zircaloy-4", Zirconium in the Nuclear Industry: Tenth International Symposium, ASTM STP 1245, A.M. Garde and E.R. Bradley, Eds., American Society for Testing and Materials, Philadelphia, 1994, pp. 351-377.
3. T. Kido and K. Ranta-Puska, Zircaloy Corrosion at High LiOH Concentration under PWR Conditions (IFA-568.1 Final Report), OECD Halden Reactor Project Report, HWR-333, October 1992.
4. Torill Karlsen and Carlo Vitanza, "Effects of Pressurized Water Reactor (PWR) Coolant Chemistry on Zircaloy Corrosion Behavior", Zirconium in the Nuclear Industry: Tenth International Symposium, ASTM STP 1245, American Society for Testing and Materials, West Conshohocken, PA, 1994, pp. 779-789.
5. M.V. Polley, H.E. Evans, P.O. Andersson and J. Larsson, "Effect of Lithium Hydroxide on Zircaloy Corrosion in the Ringhals-3 PWR Plant", EPRI Report, EPRI TR-100389, Project 2493-5 (March 1992).
6. B. Cheng, P.M. Gilmore and H.H. Klepfer, "PWR Zircaloy Fuel cladding

- Corrosion Performance, Mechanisms and Modeling”, Zirconium in the Nuclear Industry : Eleventh International Symposium, ASTM STP 1295, E.R. Bradley and G.P. Sabol, Eds., American Society for Testing and Materials, 1996, pp. 137-160.
7. S. Levy, “Forced convection subcooled boiling – prediction of vapor volumetric fraction”, International Journal of Heat and Mass Transfer, Vol. 10 (1967) pp951-965
 8. C.L. Wheeler, C.W. Stewart, R.J. Cena, D.S. Rowe, and A.M. Sutey, “COBRA-IV-I: An interim version of COBRA for thermal hydraulic analysis of rod bundle nuclear fuel elements and cores”, BNWL-1962.
 9. B. Cox, M. Ungurelu, Y.M. Wong and C. Wu, “Mechanisms of LiOH Degradation and H_3BO_3 Repair of ZrO_2 Films”, Zirconium in the Nuclear Industry : Eleventh International Symposium, Garmisch-Partenkirchen, Germany, September 11-14, 1995.
 10. P. Billot, J. Robin, A. Giordano, . Peybernes, J. Thomazet and H. Amalrich, "Experimental and Theoretical Studies of Parameters that Influence Corrosion of Zircaloy-4", Zirconium in the Nuclear Industry: Tenth International Symposium, ASTM STP 1245, American Society for Testing and Materials, West Conshohocken, PA, 1994, pp. 351-377.
 11. Y.H. Koo, B.H. Lee, and D.S. Sohn, “COSMOS: A computer code for the analysis of LWR UO_2 and MOX fuel rod”, Journal of the Korean Nuclear Society, Vol. 30, (1998) 541
 12. Otto A. Besch, S.K. Yagnik, K.N. Woods, C.M. Eucken, and E. R. Bradley, “Corrosion behavior of Duplex and reference cladding in NPP Grohnde”, Paper presented at the Eleventh International Symposium on Zirconium in the Nuclear Industry, Garmisch-Partenkirchen, Germany, September 11-14, 1995.
 13. A.R. Massih and P. Rudling, "Corrosion behavior of Zircaloy-2 and Zircaloy-4 Claddings in Pressurized water reactors”, Proceedings of the ANS International Topical Meeting on Light Water Reactor Fuel Performance, Avignon, France, April 21-24, 1991, pp. 716.

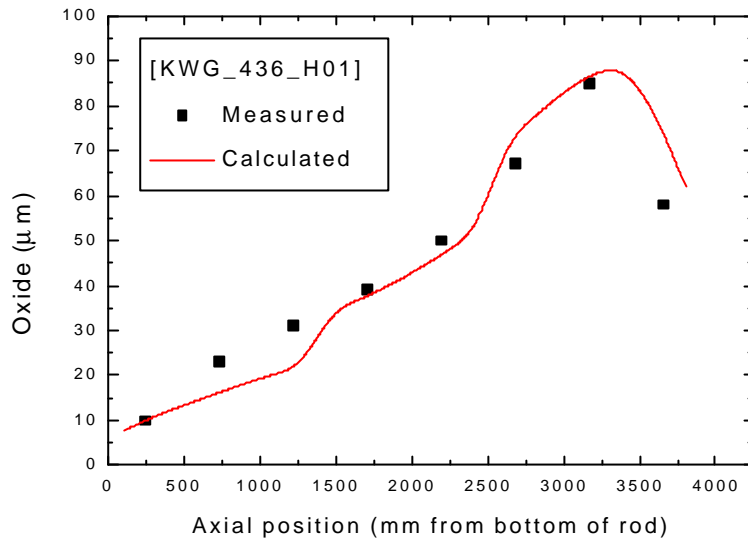


Fig. 1 Comparison of calculated and measured oxide thickness for KWG_436_H01 (Standard).

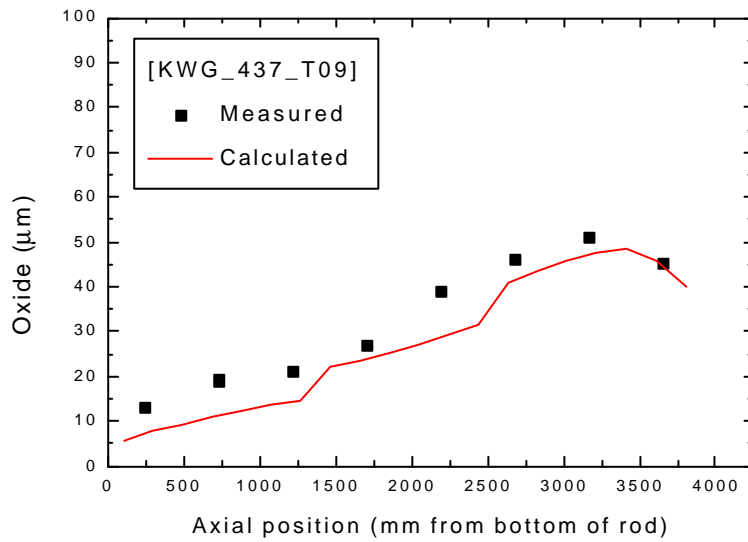


Fig. 2 Comparison of calculated and measured oxide thickness for KWG_437_T09 (low Sn).

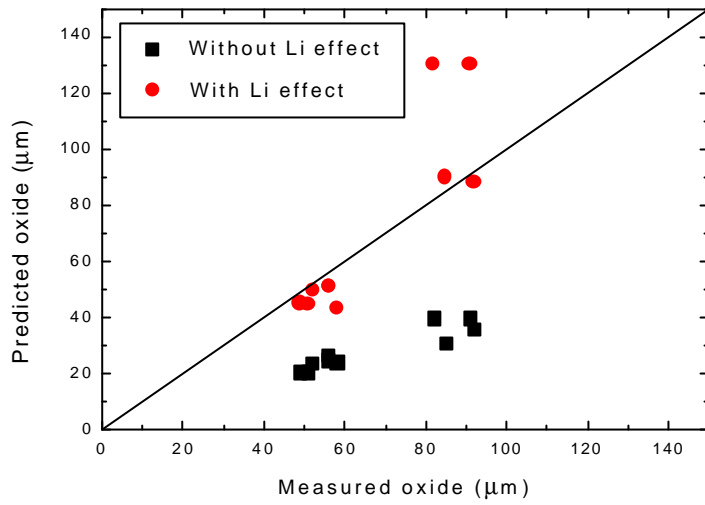


Fig. 3 Comparison of oxide thickness showing the lithium effect.

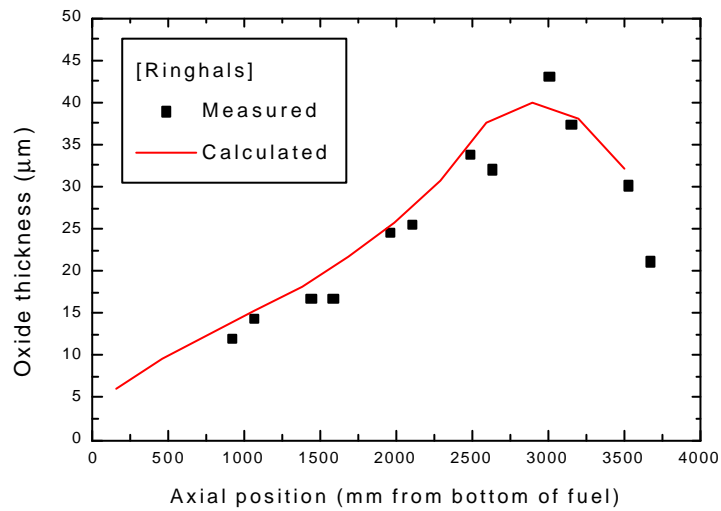


Fig. 4 Comparison of calculated and measured oxide thickness for RINGHALS-3.

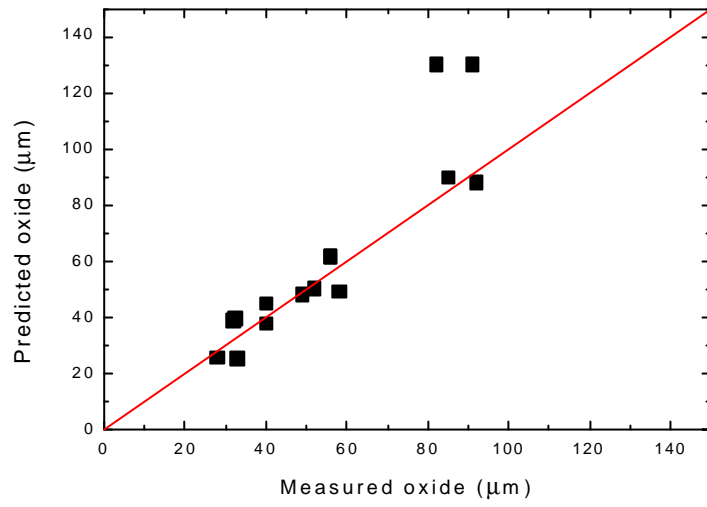


Fig. 5 Comparison of calculated and measured oxide thickness from GROHNDE and RINGHALS-3 database.